Hydraulic Flow and Vascular Clearance Influences on Intravitreal Drug Delivery

Paul J. Missel[1,2]

Received June 14, 2002; accepted July 31, 2002

Purpose. A recent paper proposed a model for hydraulic flow in the eye, claiming this could affect intravitreal drug administration. The impact of flow on various modes of administration was investigated in a physiologically accurate ocular model of the rabbit eye.

Methods. Hydraulic flow initiated at the hyaloid was simulated in a three-dimensional finite element model including effects of convection and episcleral efflux. The interrelation between hydraulic and vascular clearance was treated using a method in which choroidal clearance is effected by simple boundary conditions, diminishing computing requirements. Drug diffusion coefficient and clearance rates for the choroid and anterior chamber were varied.

Results. Volumes and velocities of fluid flow permeating the vitreous agreed with literature values. Hydraulic flow impacted clearance of compounds not eliminated by the choroid; agreement with experimental data justified assuming perfect aqueous humor mixing. Hypertensive pressure produced up to a maximum 4-fold change in vitreal drug content from an intravitreal device depending upon location, orientation of the releasing surface, but was less important than vascular clearance strength and diffusion coefficient.

Conclusions. The influence of intraocular pressure (IOP)-induced hydraulic flow is not likely to be of clinical significance for low molecular weight drugs that are efficiently cleared by the choroid.

KEY WORDS: intravitreal drug delivery; Darcy's law; hydraulic flow; vascular clearance;

INTRODUCTION

A recent study (1) measured the hydraulic permeability of ocular tissue and commented on the impact of Intraocular pressure (IOP) induced hydraulic flow on intravitreal drug transport. Using a unidimensional model, they concluded flow-induced convection accounts for up to 30% of drug transport. Previous studies neglected convection (2–6). It has been reported (7) that posterior juxtascleral administration of AL-3789 (Anecortave Acetate, 4,9(11)-pregnadien-17A,21-diol-3,20-dione-21-acetate, CAS Registry Number 7753-60-8, molecular weight 386) is effective for treating age-related macular degeneration. It was desired to estimate whether or not hydraulic effects would also be important when modeling delivery from simulated intravitreal devices.

Simulations are carried out over a range of pressure using simple boundary conditions applied to selected surfaces of a three-dimensional (3-D) ocular structure. Vascular clearance by the choroid was also simulated. A previous study (8) showed the influences of hydraulic and vascular effects can interact rather intricately. This approach is now extended to 3-D, and the impact of placement of the device can be elucidated. Literature studies have been used to compare predictions of the hydraulic model.

METHODS

Software

Symbolic manipulations to derive closed-form expressions were assisted by Macsyma version 2.4 for Windows (Macsyma, Inc., copyright 1999) (www.ma.utexas.edu/users/wfs/maxima.html, accessed 10/02/02). Finite element simulations were conducted using FlexPDE (PDE Solutions; P.O. Box 4217, Antioch, Calif., www.pdesolutions.com), version 3.01f1, as used previously when simulating tissue partitioning (9).

Equations

Ignoring at first vascular effects, the concentration variable C and each of the vectorial components for the velocity appear in the convective diffusion equation:

$$\mathrm{div}(D\ \mathrm{grad}(C)) - \vec{V} \cdot \mathrm{grad}(C) = \mathrm{dt}(C) \qquad (1)$$

where D is the diffusion coefficient and $\vec{V}$ is the velocity vector (time dependence ignored for steady state). Fluid velocity is obtained by solving for creeping flow in a porous

[1] R2-45, Drug Delivery, Alcon Research Ltd., 6201 South Freeway, Fort Worth, Texas 76134.

[2] To whom correspondence should be addressed. (e-mail: paul.missel@alconlabs.com)

ABBREVIATIONS: PDE, FEM, Partial Differential Equation, Finite Element Method; 1-D, 2-D, 3-D, One-Dimensional, Two-Dimensional, Three-Dimensional; r, three-dimensional spatial coordinate (M); r_0, r-coordinate where the vitreous begins in the reference model (M); r_1, r-coordinate of the vitreous/choroid boundary in the reference model (M); r_2, r-coordinate of the outer scleral boundary of the reference model (M); δ, thickness of the vascular layer (choroid) (M); C, Concentration of diffusant (variable submitted to finite element method) (Kg/M^3); C_b, concentration of diffusant (actual physical concentration) (Kg/M^3); C_{fin}, concentration predicted by the finite vascular (choroid) model (Kg/M^3), comprised of $C_1(r)$ in the vitreous, $C_2(r)$ in the choroid, and $C_3(r)$ in the sclera; C_{inf} concentration predicted by the infinitesimal vascular model (Kg/M^3), comprised of $C_4(r)$ in the vitreous and $C_5(r)$ in the entire region beyond the vitreous; D_n, diffusion coefficient for drug in region n (1- vitreous, 2-choroid, sclera) ($M^2\ s^{-1}$); P_0, parameter reflecting strength of vascular clearance for the infinitesimal vascular model, applied as boundary condition outside the vitreous ($M\ s^{-1}$); P_h, parameter reflecting strength of clearance by aqueous humor turnover, applied as boundary condition on the hyaloid membrane annulus (Ms^{-1}); β, parameter reflecting strength of vascular clearance for the finite vascular model; applied as a sink to the convective diffusion equation in the vasculature ($s^{-1/2}$); p, pressure variable (Pa); p_{inlet}, value of hydrostatic pressure in excess of the episcleral venous pressure (Pa); $p_{1,2}$, hydrostatic pressure in region 1, 2 of the reference model (Pa); $a_{1,2}$, $b_{1,2}$, coefficients for r-dependence of pressure in region 1,2 (Pa M, Pa); V_f, velocity of fluid (aqueous humor) percolating through the system ($M\ s^{-1}$); $K_{h,n}$, hydraulic conductivity of region n (units of length^2 expressed already having been divided by the percolating fluid viscosity assuming the viscosity of water); J_n, parameter combining hydraulic and diffusive properties of region n (M); ν, combines hydraulic, diffusive properties of region 2 and vascular clearance (-); k_v, elimination rate of drug from the vitreous after bolus injection (s^{-1}); γ, concentration ratio, inner sclera / outer vitreous (infinitesimal choroid model); (–), μ, permeating fluid viscosity (Pas).

0724-8741/02/1100-1636/0 © 2002 Plenum Publishing Corporation

medium. Using Darcy's law, the local volume flux rate of fluid is related to the local pressure gradient by the equation (10):

$$\vec{V} = -\frac{K_h}{\mu}\,\mathrm{grad}(p) \tag{2}$$

where p is the scalar pressure variable, K_h is the permeability of the porous medium to fluid flow and μ is the fluid viscosity. Assuming conservation of matter, $\mathrm{div}(\vec{V}) = 0$ (11), thus:

$$\mathrm{div}\left(\frac{K_h}{\mu}\,\mathrm{grad}(p)\right) = 0 \tag{3}$$

Solution Schema

Eqs (1) and (3) are submitted to the finite element method by one of two schemas:

(1) Time-Dependent Simulations. Pressure is determined by solving Eq (3) subject to regional hydraulic conductivity and boundary conditions. The fluid velocity resulting from Eq (2) is imported into a separate procedure solving Eq (1) subject to regional diffusion properties and concentration boundary conditions.

(2) Steady-State Simulations. Eqs (1) and (3) are solved simultaneously, applying all regional property assignments and boundary conditions for both pressure and concentration at once.

Problem Geometry/Materials Properties

The mesh was constructed to represent the rabbit posterior chamber, with a device placed either 1) near the hyaloid or 2) behind the lens (Fig. 1a). The side device resembles the Vitrasert (12) and is similar to the placement in previous studies (3,6). The central device has been proposed recently (5). Half the ocular sphere was constructed, cut along the symmetry plane. Ocular dimensions are from reference (2). The thickness of the sclera was set to a uniform value of 0.3 mm as assumed in reference (1). Fig. 1 illustrates the fluid velocity distribution obtained. Regional property assignments are given in Table I. The vitreal diffusion coefficient for Fluorescein was taken from Reference 13. Polymer diffusion coefficients were calculated using 6×10^{-11} M^2 s^{-1} for 67 kD Dextran (14) and assuming diffusivity scales with the cube root of the molecular mass. Scleral diffusion coefficients were set to a value of $1/6^{th}$ the corresponding vitreal value, consistent with estimates from transport studies through the sclera for small (15) and large (16) molecules, except as indicated.

Boundary Conditions

15 or 25 mmHg pressure is applied to the hyaloid, simulating normotensive and hypertensive pressures. Outer scleral pressure (episcleral venous pressure) was 10 mmHg; the 5 mmHg drop is comparable to rabbits (17,18) and humans (19). A condition (1.16×10^{-8} Kg / M^2 - s) was applied to the releasing surface (circular area 1×10^{-6} M^2) producing a drug flux of 1 μg /day. Drug and fluid flux were prohibited through every other surface of the device and the lens (fluid flux also prohibited from the releasing surface). Drug is eliminated by the anterior pathway, choroidal clearance, and episcleral outflow. Anterior clearance is effected by setting the normal derivative of concentration to $-P_h$ C, where

$$P_h \equiv f/A_h \tag{4}$$

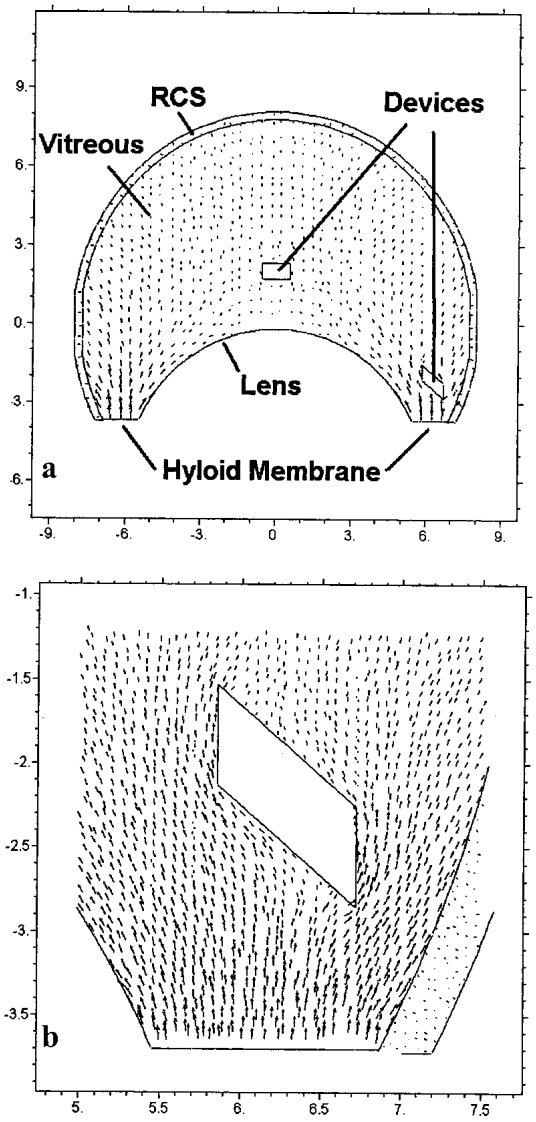

Fig. 1. a) Cross-sectional view of the rabbit geometry showing the placement of intravitreal devices. Vectors indicate direction and velocity of permeating fluid; maximum length arrow corresponds to 6×10^{-8} M s^{-1}. Dimensions are in mm. b) Close-up of one of the devices.

Table I. Materials Properties Assignments

	Diffusion coefficient M^2 s^{-1}	Hydraulic conductivity cm^2/(Pa s)
Vitreous	Denoted DC_v	$K_{h,v}/\eta = 8.4 \times 10^{-7}$
	Fluorescein 6.0×10^{-10}	(Reference 1)
	Dextrans:	
	10.5 kD 1.1×10^{-10}	
	67 kD 6.0×10^{-11}	
	157 kD 4.5×10^{-11}	
Sclera	Denoted DC_s	$K_{h,s}/\eta = 1.5 \times 10^{-11}$
	$DC_s = DC_v/6$ unless indicated otherwise	(Reference 26)

where A_h is the hyaloid area (6×10^{-5} M^2) and f is the turnover rate of aqueous humor, 3.7–6 $\times$ 10^{-11} M^3 s^{-1} (20,21). Assuming the aqueous compartment to be well mixed, P_h was set to 8×10^{-7} M s^{-1} for steady state simulations. The normal derivative of concentration on the outer sclera is set to $-V_{f,normal}$ C $*$ γ, where γ is the ratio of drug concentration of the inner sclera divided by that of the outer vitreous, the fraction of drug surviving choroidal clearance (γ becomes smaller as P_0 becomes larger). The functional dependence of γ upon P_0 is derived in the appendix, and represents an extension of the method developed previously for planar geometry (8), in which the impact of the choroid is represented by imposing a concentration discontinuity (the infinitesimal choroid model). The infinitesimal model was developed in order to conserve memory and CPU requirements for the 3-D simulations. A reference problem, consisting of either two or three concentric shells representing an idealized spherical eye, is solved exactly to derive the method and to elucidate the interaction of vascular and hydraulic clearance.

Bolus Injection Simulations

The initial condition was a 0.5 μL spherical bolus behind the lens on the symmetry axis, allowing use of cylindrical coordinates; solution scheme 1) was used. Since the materials whose vitreous clearance was simulated were not cleared by the choroid (14,21), vascular clearance was not included. The hyaloid clearance rate was varied from 10^{-8}–10^{-5} M s^{-1}, to investigate the impact of transfer efficiency across the hyaloid. The natural logarithm of the total drug in the vitreous was regressed against time for the terminal phase of elimination to determine the elimination rate k_v. For Fluorescein, the period of time regressed was 12–24 h after the initial condition, with 1.2 h timesteps; for polymers the regression was carried out over 3–14 days, with ½ day timesteps. Convergence is achieved in about 150 timesteps consuming 30 min CPU time (Pentium III 600 MHz).

Standard Reference Problem Simulations

The domain consists of either two or three concentric shells: vitreous (3–7.8 mm), choroid (thickness 0.1 mm, if present), and sclera (out to 8.1 mm). Material properties and boundary conditions are in the Appendix. The pressure drop (inner vitreous to outer sclera) was 15 mmHg. When the choroid region was included (the finite choroid model), the convective diffusion equation contains the term β^2 C (see Equation A-8); the value of β in the choroid was set from the value of P_0 using Eq (A-11). Expressions for the finite choroid model were used to define the initial values for the concentration variable, and the initial value for pressure was set to p $= p_{inlet}$ everywhere. Three stages were used to arrive at the solution: 1) zero fluid velocity and vascular clearance large ($\beta = 0.1$); 2) nonzero fluid velocity and vascular clearance large ($\beta = 0.1$); 3) nonzero velocity and vascular clearance relaxed to its intended value. The outcome of each stage was used to provide initial estimates for the beginning of the succeeding stage. About 4–6 cpu minutes were required for convergence (longer time for the finite choroid model) to obtain agreement with the exact solution to within < 0.1%. The reference problem for the infinitesimal choroid model was also solved in 3-D Cartesian geometry, to provide an estimate for the accuracy of FlexPDE for the geometry that would be required for solving the off-axis device problem; agreement was obtained to within 0.5% with about 15 min CPU time.

Simulations for Intravitreal Devices

All device problems were solved in 3-D Cartesian geometry. Simulations were carried out for all four device configurations (central forward, central rearward, side forward, and side rearward releasing) with applied pressure difference (hyaloid to outer sclera) of 0, 5, and 15 mmHg. The hyaloid clearance P_h was set to the well-stirred value, and the vascular clearance rate P_0 was varied over the range 10^{-10} – 10^{-4} M s^{-1} to simulate drugs having a range of vascular clearance properties. Convergence was achieved in 15–45 min CPU time.

RESULTS AND DISCUSSION

Pressure

The vast difference in hydraulic conductivity between vitreous and sclera produces a nearly uniform pressure distribution in the vitreous and a steep ramplike dropoff to zero across the sclera along outward radial paths.

Fluid Velocity

Vectors plotted in Fig. 1 depict flow direction and magnitude. Flow is highest near the hyaloid inlet and diminishes as fluid is diluted in the vitreous. Maximum velocities occur along surface boundaries; for example, the abrupt drop between the outer vitreous and the inner sclera at the hyaloid. Fig. 1b illustrates velocity tends to be higher adjacent to device surfaces. This is the result of not specifying no-slip boundary conditions as is done for the full Navier-Stokes equation (22). We can only impose boundary conditions on pressure and must live with whatever consequences this has on velocity. More complicated methods beyond the scope of this paper (23) would be required to improve upon this. The integral of flow of fluid across the hyaloid membrane (no device) at 5 mmHg applied pressure drop is 1.9×10^{-12} M^3 s^{-1} (0.11 μl min^{-1}), 3-5% of the aqueous humor production, comparable to experimental estimates (13,24) for the rate of fluid seepage from the aqueous to the vitreous compartments in the rabbit eye of 0.1–0.13 uL min^{-1}. The fluid velocity directed outward through the retina at the posterior pole is 3.5 $\times$ 10^{-9} M s^{-1}, comparing favorably with the experimental estimate (13) of 3.9×10^{-9} M s^{-1}.

Clearance Rates after Bolus Injections

Fig. 2 summarizes the bolus injection studies. Target windows indicate expected clearance rates k_v. Target vertical expanse is determined by the uncertainty in k_v (14,21), horizontal expanse by the uncertainty in P_h assuming perfect aqueous mixing. Clearance is diffusion limited beyond 10^{-7} M s^{-1}. Setting scleral diffusion to be $1/6^{th}$ that in the vitreous (top four curves), simulations come close to the desired targets, agreement being less good for larger polymers. Scleral diffusion for larger polymers might be much slower. Simulations for 157 kD hit the target if scleral diffusivity is reduced to $DC_v/100$; material available for episcleral efflux is reduced. Further decreases in DC_s do not produce slower clearance rates; at this

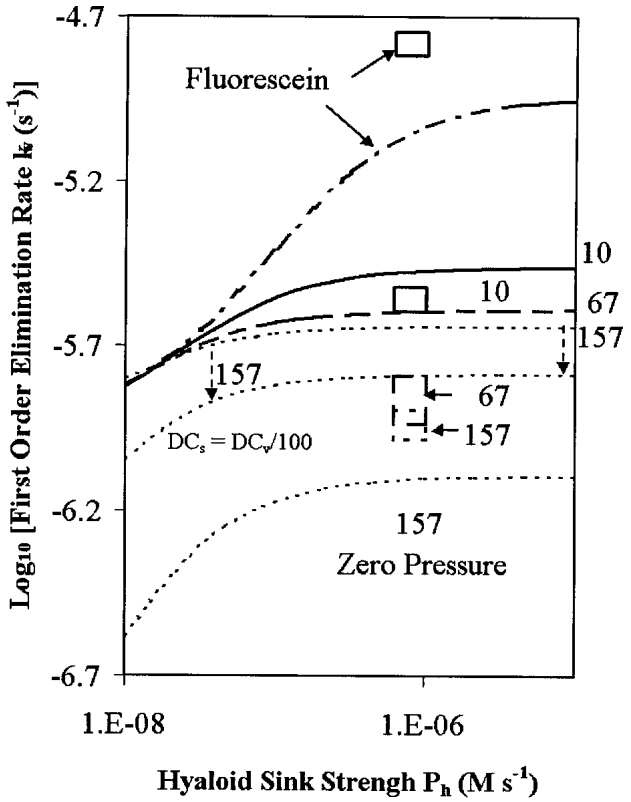

Fig. 2. Simulations of intravitreal bolus injections for compounds that are not cleared by the choroidal vasculature plotted vs. the strength of the hyaloid clearance boundary condition P_h. (_ . _) Fluorescein in the presence of an uptake inhibitor; (___) 10.5 kD Dextran; (__ __) 67 kD Dextran; (- - -) 157 kD Dextran. Also shown for the latter is the impact of reducing the diffusion coefficient in the sclera to 1/100th that in the vitreous (central dashed curve) and the effect of neglecting hydraulic flow (lowest dashed curve). Target boxes indicated are from the literature data and assume first-order elimination by perfect mixing in the anterior chamber.

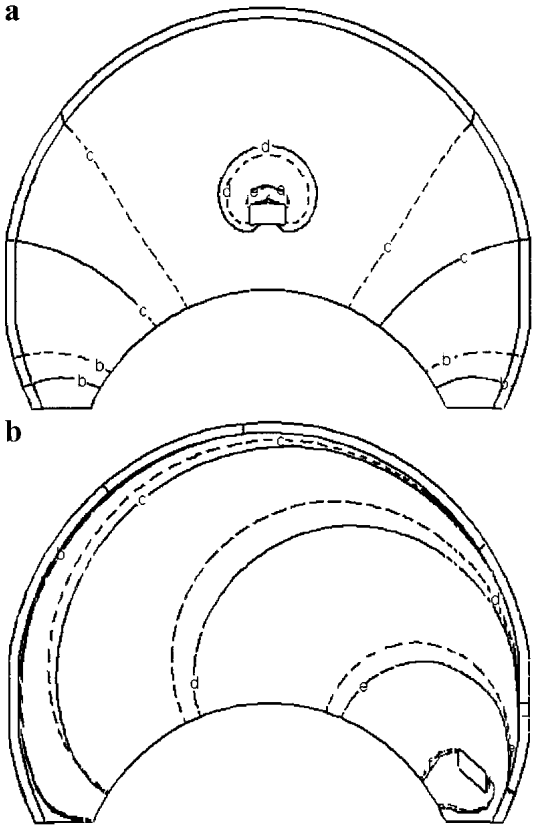

Fig. 3. Contour plots of log of concentration at steady state; solid contours are for zero pressure, dashed for 5 mmHg. a) Central device releasing toward the retina, $P_0 = 10^{-8}$ cm s^{-1}; contours represent changes of 0.3 decadic log units, contour c corresponds to 10^{-3} Kg M^3. b) Side device releasing toward the hyaloid, $P_0 = 10^{-6}$ cm s^{-1}; contours represent changes of 1 log unit, contour e corresponds to 10^{-3} Kg M^3.

value of DC_s, transport through the sclera is effectively halted. The importance of convection is confirmed by the curve for zero hydraulic flow (lowest), which falls significantly below the target. There may come a point where further increases in molecular weight may fail to increase drug residence because the balance shifts from diffusion to convection. (Note that the value of DC_s is immaterial in the case of zero pressure and zero vascular clearance, since the sclera under these circumstances is passive to the clearance process.) Thus, in the absence of vascular clearance, the hydraulic effects of the model are confirmed, and the use of a simple boundary condition P_h to represent anterior clearance, and its numerical magnitude, are justified by the experimental data.

Steady-State Concentration in the Vitreous from an Intravitreal Device

Fig. 3 shows concentration at steady state for zero pressure (solid) and 5 mmHg (dashed) for each device. Increasing pressure pushes contours away from the hyaloid. Contours are perpendicular to the retina when clearance by the choroid is much slower than from the hyaloid (Fig. 3a), and parallel to the retina when the opposite is true (Fig. 3b).

Influences of vascular clearance, pressure, diffusivity, device placement and orientation on the steady state vitreous drug content can be elucidated from Fig. 4. The net impact of pressure is to restrict the dynamic range of vitreous drug content to within narrower limits. Transport-limiting situations occur at either extreme of vascular clearance. Once P_0 increases beyond a given value (which depends upon the vitreous diffusivity), transport becomes diffusion limited. In the limit of low P_0, clearance becomes dominated by anterior losses, held fixed by P_h. Anterior losses dominate the faster the diffusivity. Drug content for fast diffusing molecules efficiently cleared by the choroid ($P_0 > 10^{-6}$ cm s^{-1}) is independent of pressure. For compounds like Fluorescein (clearance estimates ranging from 2.3–5.5 $\times$ 10^{-5} cm s^{-1} (13,25)), the effect of pressure can be ignored. Pressure becomes important only for drugs not efficiently cleared by the choroid, more so for slow diffusivity, with effects ranging from 40–75% depending on device placement/orientation, with more intriguing profiles occurring from side placement. The subtle behavior of the curves in Fig. 4 is confirmed from the results of the standard reference problem (Appendix, Fig. A-3). The only difference is that the reference problem did not include anterior clearance; thus, in the absence of hydraulic pressure, drug content increased ad infinitum. The lack of effect of pressure for small molecules that are effectively cleared and the inflection points is reproduced.

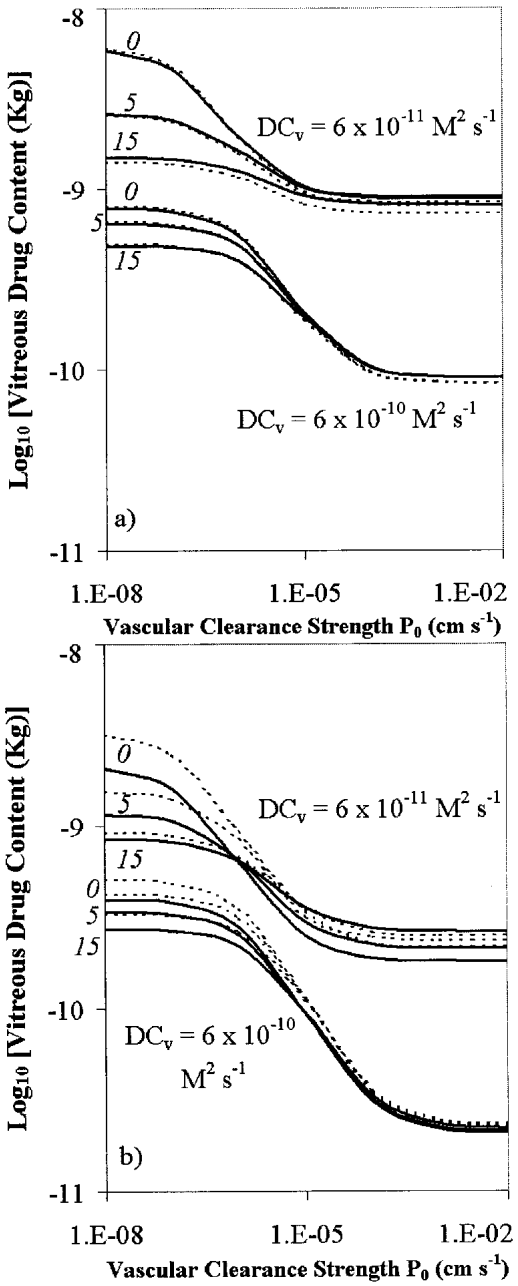

Fig. 4. Total drug content of the vitreous hemisphere at steady state vs. vascular clearance strength P_0. Solid curves: Device releasing toward the front; dashed curves: device releasing toward the retina. Simulations were conducted at 0, 5, or 15 mmHg applied pressure as indicated in italics. a) Central placement; b) side placment.

Steady-State Drug Content of the Sclera

Although not designed to match concentration in the choroid, the infinitesimal choroid model provides a fair assessment of drug content in the sclera. For fast diffusers, predictions of scleral drug content from either choroid model agree to within 90% for the entire range of $0.001 < \beta < 1$. For slow diffusers, agreement is within 90% over the narrower range $0.001 < \beta < 0.1$. $\beta = 0.1$ corresponds to $P_0 = 3 \times 10^{-5}$ cm s^{-1}, comparable to the value for Fluorescein. Thus, the infinitesimal choroid model underestimates the drug content of the sclera for large drugs that are cleared comparable to or less efficiently than Fluorescein by less than 10%, with better agreement for small drugs.

CONCLUSION

Flow predicted through the vitreous is so small that it contributes to diffusion only for large molecules or for small molecules not efficiently cleared by the choroid. The effect is greatest near the hyaloid, the fluid inlet, where velocity is highest. Exterior efflux can be as important as convection. This became apparent in the bolus studies; when the convective term was left out of the diffusion equation and the scleral efflux condition was still applied, the clearance rate was still increased significantly for large molecules.

There is some question regarding the unphysicality of nonzero permeating fluid velocity at tissue interfaces. Fluid velocity peaks at the pressure inlet along both hyaloid/lens and hyaloid/ sclera boundaries, also along device surfaces. Since fluid velocity is extremely small, momentum transfer represented by nonzero tangential velocity is negligible. Darcy's law flow velocity is not true local velocity but rather averaged mass flux. The device is stylistic only, having neglected the attachment tab that would influence flow. If the tangential velocity is zero at interfaces, current predictions would represent overestimates of the flow effect on steady-state drug concentration. Its influence on concentration is small for normotensive pressure even allowing for tangential fluid velocity. The fact that it may be overestimated because of this error, together with the low impact of the effect, support the idea that flow can be neglected entirely as being unlikely to have clinical significance for quickly diffusing drugs.

Perhaps of more benefit from this study is the principle of estimating vascular clearance effects—understanding their interaction with hydraulic flow, or the ability to determine the relationship between regional vs. boundary condition clearance in the absence of flow. The infinitesimal choroid model allows predictions of drug content in tissue layers beyond the choroid, where previous models have been limited to following descriptions of the vitreous cavity. This facility will be especially important were one to adapt this approach to simulating other modes of administration even more intimately involved with vasculature, such as transdermal or intracranial delivery.

ACKNOWLEDGMENT

Tony Adamis alerted me to the work of Victor Barocas who was kind enough to provide insight into the work of reference (1). Comments provided by George Bergantz (University of Washington) on CFD Online helped gain a better understanding of the physical meaning of velocity in Darcy's law flow. The assistance of Dr. Robert Nelson, PDE Solutions, Inc., was useful for tuning the finite element scripts used. Dr. Jamieson C. Kiester of 3M, Saint Paul, Minn. provided helpful insights into the mathematics of this diffusion problem and the importance of accounting for the influence of vascular effects.

APPENDIX

Standard Reference Geometry

The domain consists of a vitreous shell encapsulated by a choroidal shell, and, outermost, the sclera (see Fig. A-1a). Pressure and input drug flux conditions are applied at the innermost boundary, representing the hyaloid and device. Zero pressure is applied to the outermost boundary, where hydraulic-assisted drug efflux occurs. Two models for simulating choroidal effects are used. In the finite choroid model, clearance is effected by the sink term $\beta\ ^2C$ in the convective diffusion equation. Drug concentration varies continuously across the domain (Fig. A-1b). In the infinitesimal choroid model, clearance is effected by applying a boundary condition at the outer vitreous, and by imposing a discontinuity on physical concentration matching the finite choroid model. Materials properties appropriate for each situation, including sink conditions where applicable are:

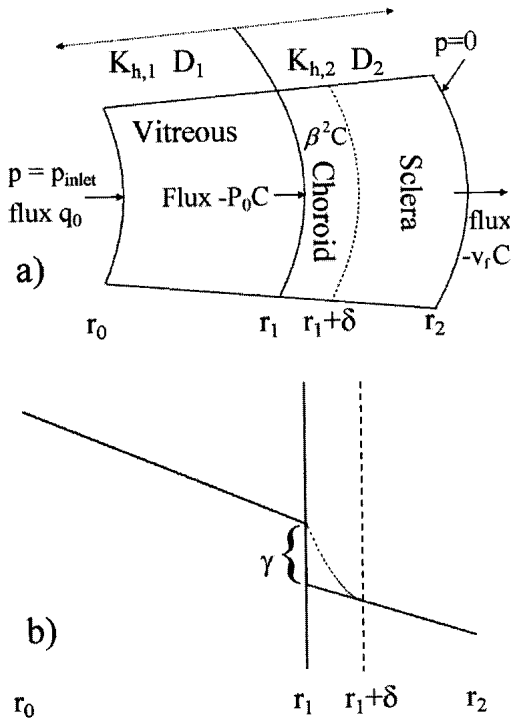

Fig. A-1. a) Problem domain, sub-domains, regional materials properties assignments and boundary conditions for the spherically symmetric reference problem; the small wedge portion shown is not to scale. Hydrostatic (intraocular) pressure and input drug flux conditions are applied to the innermost boundary, representing the hyaloid membrane and an intravitreal device. Zero pressure is applied to the outermost boundary, where hydraulic-assisted drug efflux occurs through the outer sclera. The vascular clearance is effected by assigning a sink term $\beta\ ^2C$ to the convective diffusion equation in the choroid region (finite choroid model) or by applying a flux boundary condition to the outer vitreous boundary (infinitesimal choroid model). b) Sample elevation plots for physical concentration along a path normal to the spherical surfaces. (_ _ _) Finite choroid model varies continuously across the entire domain. (____) Infinitesimal choroid model imposes a discontinuity, γ in the concentration at the outer vitreous boundary, calculated to match the results of the finite choroid model.

Finite Choroid

$D = D$	$K_h = K_{h,1}$	No Sink	$0 < r < r_1$
$D = D_2$	$K_h = K_{h,2}$	Sink $= \beta^2 * C$	$r_1 < r < r_1 + \delta$
$D = D_2$	$K_h = K_{h,2}$	No sink	$r_1 + \delta < r < r_2$

Infinitesimal Choroid

$D = D_1$	$K_h = K_{h,1}$	$0 < r < r_1$
$D = D_2$	$K_h = K_{h,2}$	$r_1 < r < r_2$

where D_1 and D_2 and $K_{h,1}$ and $K_{h,2}$ are the diffusion and hydraulic coefficients in the vitreous and sclera, respectively. Boundary conditions (apart from matching concentration/flux internally) are as follows:

Finite Choroid

$p = p_{inlet}$	flux $= q_0$	$r = r_0$
$p = 0$	flux $= V_f{*}C$	$r = r_2$

Infinitesimal Choroid

$p = p_{inlet}$	flux $= q_0$	$r = r_0$
Added sink	flux $= P_0{*}C$	$r = r_1$
$p = 0$	flux $= V_f{*}C$	$r = r_2$

We have applied the drug input at this boundary (applied here so as not to require an additional surface) to simulate delivery from an intravitreal device. The text equation Eq (3) in spherical coordinates is:

$$\frac{1}{r^2}\frac{\partial}{\partial r}\left(r^2\frac{\partial p}{\partial r}\right) = 0 \qquad \text{(A-1)}$$

providing a radial pressure dependence in each region as follows:

$$p_{1,2}(r) = \frac{a_{1,2}}{r} + b_{1,2} \qquad \text{(A-2)}$$

where $p_1(r)$ is the pressure in the vitreous and $p_2(r)$ is the pressure in the choroid/sclera. The coefficients $a_{1,2}$, $b_{1,2}$ are obtained by matching pressure and fluid flux at the appropriate boundaries as follows:

$$\text{Match pressure at } r = r_0 : \frac{a_1}{r_0} + b_1 = p_{in} \qquad \text{(A-3a)}$$

$$\text{Match pressure at } r = r_1 : \frac{a_1}{r_1} + b_1 = \frac{a_2}{r_1} + b_2 \qquad \text{(A-3b)}$$

$$\text{Match pressure at } r = r : \frac{a_2}{r_2} + b_2 = 0 \qquad \text{(A-3c)}$$

$$\text{Match velocity at } r = r_1 : -\frac{K_{h,1}}{\mu}\,\text{grad}(p_1(r))\Big|_{r=r_1} = -\frac{K_{h,2}}{\mu}\,\text{grad}(p_2(r))\Big|_{r=r_1} \qquad \text{(A-3d)}$$

where μ is the viscosity of fluid. Coefficients that simultaneously solve equations (A-3a–d) are:

$$a_1 = -\frac{K_{h,2}\, p_{in}\, r_0\, r_1\, r_2}{\Delta_p} \tag{A-4a}$$

$$a_2 = -\frac{K_{h,1}\, p_{in}\, r_0\, r_1\, r_2}{\Delta_p} \tag{A-4b}$$

$$b_1 = \frac{p_{in}\, r_0[(K_{h,2} - K_{h,1})r_2 + K_{h,1}\, r_1]}{\Delta_p} \tag{A-4c}$$

$$b_1 = \frac{K_{h,1}\, p_{in}\, r_0\, r_1}{\Delta_p} \tag{A-4d}$$

where

$$\Delta_p = r_0[(K_{h,2} - K_{h,1})r_2 + K_{h,1}\, r_1] - K_{h,2}\, r_1\, r_2 \tag{A-4e}$$

The steady-state convective diffusion equation in the vitreous and sclera becomes:

$$\frac{1}{r^2}\frac{\partial}{\partial r}\left(D_i\, r^2 \frac{\partial C_i}{\partial r}\right) = \frac{D_i J_i}{r^2}\frac{\partial C_i}{\partial r} \tag{A-5}$$

where i denotes a specific region (1 for vitreous, 2 for choroid or sclera) and where the J_i's are given by:

$$J_{1,2} \equiv \frac{K_{h,1,2}\, a_{1,2}}{\mu D_{1,2}} \tag{A-6}$$

The solution of Equation (A-5) is:

$$C_i(r) = E_i\, e^{\frac{-J_i}{r}} + F_i \tag{A-7}$$

The convective diffusion equation in effect in the choroid for the finite choroid model is:

$$\frac{1}{r^2}\frac{\partial}{\partial r}\left(D_2\, r^2 \frac{\partial C}{\partial r}\right) = \frac{D_2 J_2}{r^2}\frac{\partial C}{\partial r} + \beta^2 C \tag{A-8}$$

which though insoluble can be approximated as follows:

$$\frac{1}{r^2}\frac{\partial}{\partial r}\left(Dr^2\frac{\partial C_2}{\partial r}\right) \approx \frac{D_2 J_2}{r_1 r}\frac{\partial C_2}{\partial r} + \frac{{r_1}^2}{r^2}\beta^2 C_2 \tag{A-9}$$

This equation is readily solvable, though the solution is not particularly simple:

$$C_2(r) \equiv E_2\, r^{\left[\frac{\nu - 1 + \frac{J_2}{r_1}}{2}\right]} + F_2\, r^{-\left[\frac{\nu + 1 - \frac{J_2}{r_1}}{2}\right]},$$
$$\nu \equiv \sqrt{\frac{4\beta^2 {r_1}^2}{D_2} - \frac{2J_2}{r_1} + \frac{{J_2}^2}{{r_1}^2} + 1} \tag{A-10}$$

Thus, the appropriate expression for concentration in each region is summarized as follows:

Finite Choroid, C_{fin}

Expr1: $C_1(r) = E_1\, e^{\frac{-J_1}{r}} + F_1 \qquad r_0 < r < r_1$

Expr2: $C_2(r) \equiv E_2\, r^{\left[\frac{\nu - 1 + \frac{J_2}{r_1}}{2}\right]} + F_2\, r^{-\left[\frac{\nu + 1 - \frac{J_2}{r_1}}{2}\right]} \qquad r_1 < r < r_1 + \delta$

Expr3: $C_3(r) = E_3\, e^{\frac{-J_2}{r}} + F_3 \qquad r_1 + \delta < r < r_2$

Infinitesimal Choroid, C_{inf}

Expr4: $C_4(r) = E_4\, e^{\frac{-J_1}{r}} + F_4 \quad r_0 < r < r_1$

Expr5: $C_5(r) = E_5\, e^{\frac{-J_2}{r}} + F_5 \quad r_1 < r < r_2$

Applying boundary conditions on concentration, and matching flux/concentration at internal boundaries, the following equations are obtained, which when solved simultaneously provide the coefficients E_i, F_i:

Finite Choroid

Eq1: $-D_1 \left.\frac{dC_1}{dr}\right|_{r=r_0} = q_0$

Eq2: $C_1|_{r=r_1} = C_2|_{r=r_1}$

Eq3: $-D_1 \left.\frac{dC_1}{dr}\right|_{r=r_1} = -D_2 \left.\frac{dC_2}{dr}\right|_{r=r_1}$

Eq4: $C_2|_{r=r_1+\delta} = C_3|_{r=r_1+\delta}$

Eq5: $-D_2 \left.\frac{dC_2}{dr}\right|_{r=r_1+\delta} = -D_2 \left.\frac{dC_3}{dr}\right|_{r=r_1+\delta}$

Eq6: $-D_2 \left.\frac{dC_3}{dr}\right|_{r=r_2} = \frac{D_2 J_2}{r_2^2} C_3|_{r=r_2}$

Infinitesimal Choroid

Matching flux at $r = 0$ — Eq7: $-D_1 \left.\frac{dC_4}{dr}\right|_{r=r_0} = q_0$

Matching value at $r = r_1$ — Eq8: $C_5|_{r=r_1} = \gamma * C_4|_{r=r_1}$

Matching flux at $r = r_1$ — Eq9: $-D_1 \left.\frac{dC_4}{dr}\right|_{r=r_1} = P_o\, C_4|_{r=r_1} - D_2 \left.\frac{dC_5}{dr}\right|_{r=r_1}$

Matching value at $r = r_1 + \delta$ (absent)

Matching flux at $r = r_1 + \delta$ (absent)

Matching flux at $r = r_2$ — Eq10: $-D_2 \left.\frac{dC_5}{dr}\right|_{r=r_2} = \frac{D_2 J_2}{r_2^2} C_5|_{r=r_2}$

The quantity γ allows for a discontiuity at the vitreous/scleral boundary. Using the finite choroid model Expr1–3 above, equations [Eq1–Eq6] are solved simultaneously to obtain the coefficients E_{1-3}, F_{1-3}:

$$E_1 = -\frac{q_0 e^{\frac{J_1}{r_0}} {r_0}^2}{D_1 J_1}$$

$$F_1 = \frac{q_0 {r_0}^2 e^{\frac{J_1}{r_0} - \frac{J_1}{r_1}} \left\{ \begin{bmatrix} \left(\frac{r_1+\delta}{r_1}\right)^{\nu} (D_2((\nu+1)r_1 - J_2) + 2D_1J_1)((\nu-1)r_1(r_1+\delta) - J_2(r_1-\delta)) \\ -(D_2((\nu-1)r_1 + J_2) - 2D_1J_1)((\nu+1)r_1(r_1+\delta) + J_2(r_1-\delta)) \end{bmatrix} e^{\frac{J_2}{r_2}} \gamma_1 + \right.}{D_1 D_2 J_1 \left\{ \begin{bmatrix} \left(\frac{r_1+\delta}{r_1}\right)^{\nu} ((\nu+1)r_1 - J_2)((\nu-1)r_1(r_1+\delta) - J_2(r_1-\delta)) \\ -((\nu-1)r_1 + J_2)((\nu+1)r_1(r_1+\delta) + J_2(r_1-\delta)) \end{bmatrix} e^{\frac{J_2}{r_2}} \gamma_1 \right.}$$

$$\left. \begin{bmatrix} (D_2((\nu-1)r_1 + J_2) - 2D_1J_1)((\nu+1)r_1 - J_2) \\ -\left(\frac{r_1+\delta}{r_1}\right)^{\nu} (D_2((\nu+1)r_1 - J_2) + 2D_1J_1)((\nu-1)r_1 + J_2) \end{bmatrix} e^{\frac{J_2}{r_1+\delta}} (r_1+\delta)(\gamma_1+1) \right\}$$

$$\left. \begin{bmatrix} (r_1+\delta)((\nu+1)r_1 - J_2) e^{\frac{J_2}{r_1+\delta}} (\gamma_1+1) \\ -[(\nu+1)r_1(r_1+\delta) + J_2(r_1-\delta)] e^{\frac{J_2}{r_2}} \gamma_1 \end{bmatrix} \right\}$$

$$E_2 r^{\left[\frac{\nu-1+\frac{J_2}{r_1}}{2}\right]} = q_0 {r_0}^2 e^{\frac{J_1}{r_0} - \frac{J_1}{r_1}} \frac{\left(\left(\frac{r}{r_1}\right)^{\frac{\frac{J_2}{r_1} - 1 + \nu}{2}} \right)}{r_1 * \Delta_f}$$

$$F_2 r^{-\left[\frac{\nu+1-\frac{J_2}{r_1}}{2}\right]} = q_0 {r_0}^2 e^{\frac{J_1}{r_0} - \frac{J_1}{r_1}} \frac{\left(\left(\frac{r}{r_1}\right)^{\frac{\frac{J_2}{r_1} - 1 + \nu}{2}} \right)}{r_1 * \Delta_f} \left(\frac{r_1+\delta}{r_1}\right)^{\nu}$$

$$E_3 = \frac{-2\gamma_1 \nu q_0 {r_0}^2 r_1 \left(\frac{r_1+\delta}{r_1}\right)^{\frac{\frac{J_2}{r_1}+1+\nu}{2}} e^{J_2\left(\frac{1}{r_2} + \frac{1}{r_1+\delta}\right) + J_1\left(\frac{1}{r_0} - \frac{1}{r_1}\right)}}{\Delta_f}$$

$$F_3 = \frac{2(\gamma_1+1)\nu q_0 {r_0}^2 r_1 \left(\frac{r_1+\delta}{r_1}\right)^{\frac{\frac{J_2}{r_1}+1+\nu}{2}} e^{\frac{J_2}{r_1+\delta} + J_1\left(\frac{1}{r_0} - \frac{1}{r_1}\right)}}{\Delta_f}$$

$$\Delta_f = 2(\gamma_1+1)\beta^2 {r_1}^3 (r_1+\delta)\left[\left(\frac{r_1+\delta}{r_1}\right)^{\nu} - 1\right] e^{\frac{J_2}{r_1+\delta}} - \left[\begin{bmatrix} (2\beta^2 {r_1}^3 (r_1+\delta) + D_2J_2(J_2 - r_1))\left(\left(\frac{r_1+\delta}{r_1}\right)^{\nu} - 1\right) \\ -D_2J_2\nu r_1 \left(\left(\frac{r_1+\delta}{r_1}\right)^{\nu} + 1\right) \end{bmatrix} e^{\frac{J_2}{r_2}} \gamma_1 \right]$$

Separately, using the infinitesimal choroid expressions Expr4,5 the equations [Eq7 – Eq10] are solved simultaneously to obtain the coefficients $E_{4,5}$, $F_{4,5}$:

$$E_4 = -\frac{q_0 {r_0}^2}{D_1 J_1} e^{\frac{J_1}{r_0}}$$

$$F_4 = \frac{q_0 {r_0}^2}{D_1 J_1} \frac{e^{\frac{J_1}{r_0}} [(D_2J_2\gamma - (P_0 {r_1}^2 + D_1J_1)\gamma_1) e^{\frac{J_2}{r_2}} + (\gamma_1+1)(D_1J_1 + P_0 {r_1}^2) e^{\frac{J_2}{r_1}}]}{\Delta_i}$$

$$E_5 = \frac{q_0 {r_0}^2 \gamma}{\Delta_i} e^{\left(J_2\left(\frac{1}{r_1} + \frac{1}{r_2}\right) + \frac{J_1}{r_0}\right)} \quad F_5 = \frac{q_0 {r_0}^2 (\gamma + \gamma_2)}{\Delta_i} e^{\left(\frac{J_2}{r_1} + \frac{J_1}{r_0}\right)}$$

$$\Delta_i = e^{\frac{J_1}{r_1}} \left[\left(D_2J_2\gamma - P_0 {r_1}^2 \gamma_1\right) e^{\frac{J_2}{r_2}} + \left(\gamma_1 + 1\right) P_0 r^2 e^{\frac{J_2}{r_1}} \right]$$

The quantities γ_1, γ_2 are, for the time being 1 and γ, where γ is the discontinuity in concentration imposed at the outer vitreous boundary for the infinitesimal choroid model. Selecting quotients avoids round-off errors:

$$\left(\frac{r_1+\delta}{r_1}\right)^{\nu} = \frac{(r_1+\delta)^{\nu}}{{r_1}^{\nu}}; \quad \left(\frac{r}{r_1}\right)^{\nu} = \frac{r^{\nu}}{{r_1}^{\nu}}; \text{ etc.}$$

Distances are on the order of 10^{-3} M; the exponent ν is a few times to many times larger than unity. It is better to take the exponent of the ratio of two small numbers than to take the ratio of their exponents. This is the reason why the radial dependence in Expr2 was subsumed into the expressions for E_2 and F_2 above. To determine a relationship between P_0 and β that will apply the same sink effect on the vitreous, note that the value of the 1/r term in the vitreous is the same for both models ($E_1 = E_4$). To obtain the same value for concentration in the vitreous requires $F_1 = F_4$. An expression for P_0 can be obtained from this equality, or by solving the relationship Expr1 = Expr4 evaluated at $r = r_1$:

$$P_0 = \frac{\begin{bmatrix} \left[D_2J_2(\gamma\gamma_1(\delta r_1(\nu\varsigma-1)-r_1{}^2+\delta J_2)+r_1(\gamma_2-1)(r_1\nu\varsigma-J_2))\right]e^{\frac{2J_2}{r_2}} \\ +(2\beta^2 r_1{}^4(r_1+\delta)-D_2J_2r_1{}^2)\gamma_1{}^2 \\ +D_2J_2(r_1(\nu\varsigma+1)-J_2)-2\beta^2 r_1{}^3(r_1+\delta)r_1\gamma_1(\gamma_1+1)e^{J_2\left(\frac{1}{r_1}+\frac{1}{r_2}\right)} \\ -(D_2J_2\gamma(r_1(\nu\varsigma-1)+J_2)+2\beta^2 r_1{}^4\gamma_1)(r_1+\delta)(\gamma_1+1)e^{J_2\left(\frac{1}{r_2}+\frac{1}{r_1+\delta}\right)} \\ +2\beta^2 r_1{}^4(r_1+\delta)(\gamma_1+1)^2e^{J_2\left(\frac{1}{r_1}+\frac{1}{r_1+\delta}\right)} \end{bmatrix}}{r_1{}^2\left(e^{\frac{J_2}{r_2}}\gamma_1-e^{\frac{J_2}{r_1}}(\gamma_1+1)\right)\begin{bmatrix} e^{\frac{J_2}{r_2}}\gamma_1(r_1(r_1+\delta)(\nu\varsigma-1)-J_2(r_1-\delta)) \\ -e^{\frac{J_2}{r_1+\delta}}(r_1+\delta)(\gamma_1+1)(r_1(\nu\varsigma-1)+J_2)\end{bmatrix}} \quad \varsigma \equiv \frac{\left(\frac{r_1+\delta}{r_1}\right)^{\nu}+1}{\left(\frac{r_1+\delta}{r_1}\right)^{\nu}-1} \tag{A-11}$$

The quantity γ is the ratio of the concentration behind versus in front of the choroid occurring by vascular clearance in the limit of zero pressure. By taking the zero pressure limit we are stating that the influences of these two physiologic effects are separable, and that the influence of vascular clearance can to a good approximation be stated by taking this limit. In the limit of $J_2 \to 0$, an exact solution to Equation (A-8) is:

$$\text{Expr2,0: } C_{2,0}(r) = \frac{1}{r}\left[E_{2,0}\sinh\left(\frac{\beta r}{\sqrt{D_2}}\right)+F_{2,0}\cosh\left(\frac{\beta r}{\sqrt{D_2}}\right)\right]$$

where ,0 has been added to denote zero pressure. Zero pressure counterparts of Expr1 and Expr3 are:

$$\text{Expr1,0: } C_{1,0}(r) = \frac{E_{1,0}}{r}+F_{1,0} \qquad \text{Expr3,0: } C_{3,0}(r) = \frac{E_{3,0}}{r}+F_{3,0}$$

The coefficients $E_{1,0}$, $F_{1,0}$, etc. are determined by a similar scheme as for the case of applied pressure, evaluating Exprs1–3,0 using Eqs(1–6); only Eq6 has changed, its right hand side now being zero in the absence of applied pressure. The resulting coefficients are as follows:

$$E_{1,0} = \frac{q_0 r_0{}^2}{D_1}$$

$$F_{1,0} = \frac{q_0 r_0{}^2\begin{bmatrix} D_2(\beta^2 r_1(r_1+\delta)-D_2+D_1)\sinh\left(\frac{\beta\delta}{\sqrt{D_2}}\right) \\ +\beta\sqrt{D_2}(D_2\delta-D_1(r_1+\delta))\cosh\left(\frac{\beta\delta}{\sqrt{D_2}}\right)\end{bmatrix}}{D_1D_2r_1\Delta_{f,0}}$$

$$E_{2,0} = \frac{q_0 r_0{}^2}{\sqrt{D_2}}\frac{\begin{bmatrix} \beta(r_1+\delta)\sinh\left(\frac{\beta(r_1+\delta)}{\sqrt{D_2}}\right) \\ -\sqrt{D_2}\cosh\left(\frac{\beta(r_1+\delta)}{\sqrt{D_2}}\right)\end{bmatrix}}{\Delta_{f,0}}$$

$$F_{2,0} = -\frac{q_0 r_0{}^2}{\sqrt{D_2}}\frac{\begin{bmatrix} \beta(r_1+\delta)\cosh\left(\frac{\beta(r_1+\delta)}{\sqrt{D_2}}\right) \\ -\sqrt{D_2}\sinh\left(\frac{\beta(r_1+\delta)}{\sqrt{D_2}}\right)\end{bmatrix}}{\Delta_{f,0}}$$

$$E_{3,0} = 0$$

$$F_{3,0} = -\frac{q_0 r_0{}^2\beta}{\sqrt{D_2}\Delta_{f,0}}, \quad \Delta_{f,0} \equiv \left[(D_2-\beta^2 r_1(r_1+\delta))\sinh\left(\frac{\beta\delta}{\sqrt{D_2}}\right)-\beta\sqrt{D_2}\,\delta\cosh\left(\frac{\beta\delta}{\sqrt{D_2}}\right)\right]$$

Thus, the desired expression for γ is obtained; the infinite r_1 limit produces the planar result:

$$\gamma = \frac{C_{2,0}|_{r=r_1+\delta}}{C_{2,0}|_{r=r_1}} = \frac{\beta r_1}{\beta(r_1+\delta)\cosh\left(\frac{\beta\delta}{\sqrt{D_2}}\right)-\sqrt{D_2}\sinh\left(\frac{\beta\delta}{\sqrt{D_2}}\right)} \xrightarrow[\lim r_1\to\infty]{} \operatorname{sech}\left(\frac{\beta\delta}{\sqrt{D_2}}\right) \tag{A-12}$$

Coefficients $E_{1,0}$, $E_{3,0}$ etc., can be verified by evaluating the corresponding expressions E_1, E_3, etc. in the limit of zero pressure (J_1, $J_2 \to 0$). Zero pressure coefficients for the infinitesimal choroid model are:

$$\text{Expr4,0: } C_{4,0}(r) = \frac{E_{4,0}}{r}+F_{4,0}$$

$$\text{Expr5,0: } C_{5,0}(r) = \frac{E_{5,0}}{r}+F_{5,0}$$

$$E_{4,0} = \frac{q_0 r_0{}^2}{D_1}$$

$$F_{4,0} = \frac{q_0 r_0{}^2(D_1-P_{0,0}r_1)}{D_1P_{0,0}r_1{}^2}$$

$$E_{5,0} = 0$$

$$F_{5,0} = \frac{q_0 r_0{}^2}{P_{0,0}r_1{}^2}*\gamma_2$$

$$P_{0,0} = \frac{\sqrt{D_2}\,\mathrm{denom}_{f,0}}{\sqrt{D_2}\,r_1 \sinh\left(\frac{\beta\delta}{\sqrt{D_2}}\right) - \beta r_1(r_1+\delta)\cosh\left(\frac{\beta\delta}{\sqrt{D_2}}\right)};$$

$$\lim_{r_1\to\infty} P_{0,0} = \beta\sqrt{D_2}\tanh\left(\frac{\beta\delta}{\sqrt{D_2}}\right)$$

where the expression for $P_{0,0}$ is determined by solving the equality $F_{1,0} = F_{4,0}$.

Adaptation of the Solution for the Finite Element Method for the Infinitesimal Choroid. The variable submitted to the finite element method must be continuous across boundaries. Thus, to produce the discontinuity in concentration at the outer vitreous, we redefine the physical concentration as follows:

$$\begin{aligned} C_b &= C && r \le r_1 \\ C_b &= \gamma * C && r > r_1 \end{aligned} \qquad \text{(A-13)}$$

where C is the dependent variable in the Finite Element Method (FEM). An accurate description of how the FEM works requires that we change two of the following members of the set Eq1–Eq10:

$$\text{Eq8: } C_5|_{r=r_1} = \gamma * C_4|_{r=r_1} \rightarrow \text{Eq8}': C_5|_{r=r_1} = C_4|_{r=r_1}$$

$$\text{Eq10: } -D_2\left.\frac{dC_5}{dr}\right|_{r=r_2} = -\frac{D_2 J_2}{r_2^{\,2}} C_5|_{r=r_2} \rightarrow \text{Eq10}': -D_2\left.\frac{dC_5}{dr}\right|_{r=r_2} = -\frac{D_2 J_2}{r_2^{\,2}}\gamma\, C_5|_{r=r_2}$$

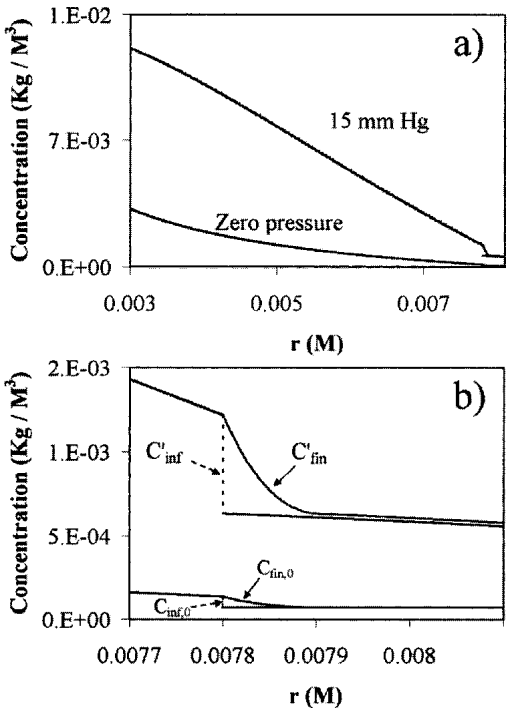

Fig. A-2. Sample prediction for the steady-state concentration profile for the situation $D_1 = 6 \times 10^{-11}$ M^2 s^{-1}, $D_2 = 1 \times 10^{-11}$ M^2 s^{-1}, and $\beta = 0.04$. The functions for both the finite and infinitesimal choroid models are compared, for both zero pressure and 15 mmHg. a) Entire domain; b) Zoom plot focusing mainly on the outer shell region.

The quantity γ is removed from Eq8. The concentration in the sclera is overestimated by the FEM by the factor γ; to provide the correct magnitude for hydraulic sink condition at the exterior sclera, this factor must be introduced into Eq10′ and also into Eq6 of the corresponding finite vascular model.

$$\text{Eq6: } -D_2\left.\frac{dC_3}{dr}\right|_{r=r_2} = -\frac{A_2 K_{h,2}}{\mu} C_3|_{r=r_2} \rightarrow \text{Eq6}': -D_2\left.\frac{dC_3}{dr}\right|_{r=r_2} = -\frac{A_2 K_{h,2}}{\mu}\gamma\, C_3|_{r=r_2}$$

All ten coefficients E_{1-5}, F_{1-5} are modified, γ appearing in many new places. These modified coefficients, denoted E_1', F_1', etc., are obtained by setting $\gamma_1 = \gamma$, $\gamma_2 = 1$ in the corresponding unprimed expression. The expression for P_0, Eq(A-11), is also modified. Figure A-2 illustrates a representative example of the radial dependence of the steady state concentration profile for the various models. The expressions used are for the FEM (γ_1 set to γ, γ_2 set to 1). The total drug in the vitreous is obtained by integrating Expr1 from $r = r_0$ to r_1:

$$\begin{aligned} M_v &= 4\pi\int_{r_0}^{r_1} r^2 C_1(r)\,dr = 4\pi\int_{r_0}^{r_1} r^2\left(E_1 e^{-\frac{J_1}{r}} + F_1\right)dr \\ &= 4\pi\int_{\frac{1}{r_0}}^{\frac{1}{r_1}} (-s^{-4})(E_1 e^{-J_1 s} + F_1)\,ds \\ &= \frac{2\pi}{3}\left\{ 2F_1(r_1^{\,3} - r_0^{\,3}) \right. \\ &\quad \left. + E_1\left[\begin{array}{c} r_1(2r_1^{\,2} - J_1 r_1 + J_1^{\,2})e^{-\frac{J_1}{r_1}} - r_0(2r_0^{\,2} - J_1 r_0 + J_1^{\,2})e^{-\frac{J_1}{r_0}} \\ + J_1^{\,3}\left(\mathrm{exp\_int}\left(-\frac{J_1}{r_1}\right) - \mathrm{exp\_int}\left(-\frac{J_1}{r_0}\right)\right) \end{array} \right] \right\} \end{aligned} \qquad \text{(A-14a)}$$

with the zero pressure limit being slightly simpler, as expected:

$$\begin{aligned} M_{v,0} &= 4\pi\int_{r_0}^{r_1} r^2 C_1(r)\,dr \\ &= 4\pi\int_{r_0}^{r_1} r^2\left(\frac{E_{1,0}}{r} + F_{1,0}\right)dr \\ &= 2\pi\left[E_{1,0}(r_1^{\,2} - r_0^{\,2}) + \frac{2}{3}F_{1,0}(r_1^{\,3} - r_0^{\,3}) \right] \end{aligned} \qquad \text{(A-14b)}$$

Figure A-3 illustrates predictions for the total drug content of the vitreous compartment versus β using Equations A-14a and A-14b. The appearance of this figure is unchanged regardless of the assignment of the value of γ_1. When γ_1 is assigned the value of γ (mimicking the FEM solution), the variation in M_v at any value of β is only slightly higher than the value predicted when γ_1 is assigned the value of unity (finite choroid solution without discontinuity). The maximum disparity is <1% for slowly diffusing and <0.3% for rapidly diffusing materials. To predict the total scleral drug content, the volume integrals are:

$$M_{s,fin} = 4\pi \int_{r_{1+\delta}}^{r_2} r^2 C_3(r)dr = 4\pi \int_{r_{1+\delta}}^{r_2} r^2 (E_3\, e^{-\frac{J_2}{r}} + F_3)dr = 4\pi \int_{\frac{1}{r_{1+\delta}}}^{\frac{1}{r_2}} (-s^{-4})(E_3\, e^{-J_2 s} + F_3)ds$$

$$= \frac{2\pi}{3}\left\{ 2F_3\,(r_2{}^3 - (r_1+\delta)^3) + E_3\left[\begin{array}{l} r_2(2r_2{}^2 - J_2 r_2 + J_2{}^2)e^{-\frac{J_2}{r_2}} - (r_1+\delta)\left(2(r_1+\delta)^2 \right. \\ \left. -J_2(r_1+\delta) + J_2{}^2\right)e^{-\frac{J_2}{r_1+\delta}} \\ +J_2{}^3\left(\text{exp\_int}\left(-\frac{J_2}{r_2}\right) - \text{exp\_int}\left(-\frac{J_2}{r_1+\delta}\right)\right) \end{array} \right] \right\} \qquad \text{(A-15)}$$

where $M_{s,fin}$ is the prediction for the content of the drug in the sclera by the finite choroid model. A similar expression for $M_{s,inf}$, the prediction for the content of the drug in the sclera by the infinitesimal choroid model, is identical to Equation A-15 with the substitution of E_5 for E_3 and F_5 for F_3. From the ratio of these expressions, making appropriate substitutions for E_3, E_5, F_3 and F_5, the following result is obtained:

$$\frac{M_{s,inf}}{M_{s,fin}} = \frac{\Delta_f \gamma\, e^{-\frac{J_2}{r_1+\delta} + \frac{J_1+J_2}{r_1}}}{2\Delta_i \nu r_1 \left(\frac{r_1+\delta}{r_1}\right)^{\frac{\left(\frac{J_2}{r_1}+\nu+1\right)}{2}}} \qquad \text{(A-16)}$$

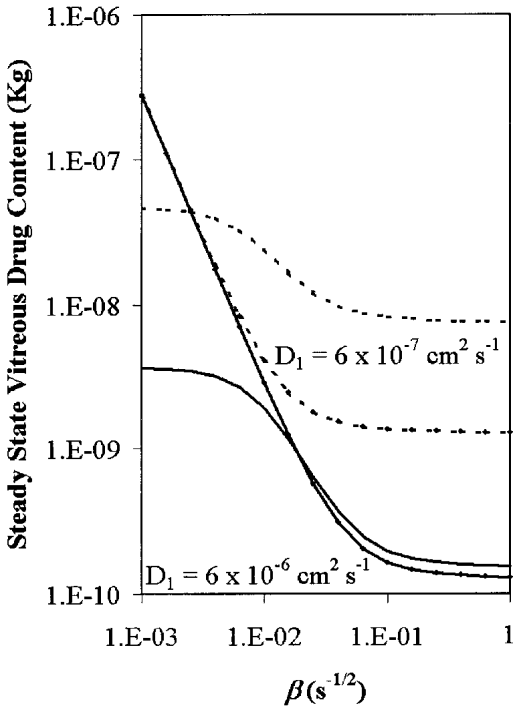

Fig. A-3. Drug content of the vitreous as predicted by Equations A-14a (for 15 mmHg) and A-14b (for zero pressure) vs. β. Solid curves: $D_1 = 6 \times 10^{-10}$ M^2 s^{-1}; dashed curves: $D_1 = 6 \times 10^{-11}$ M^2 s^{-1}; curves with added circles: zero pressure; curves alone: 15 mmHg. $D_2 = D_1/6$ throughout.

REFERENCES

1. J. Xu, J. J. Heys, V. H. Barocas, and T. W. Randolph. Permeability and diffusion in vitreous humor: implications for drug delivery. *Pharm. Res.* **17**:664–669 (2000).
2. S. Friedrich, Y.-L. Cheng, and B. Saville. Finite element modeling of drug distribution in the vitreous humor of the rabbit eye. *Ann. Biomed. Eng.* **25**:303–314 (1997).
3. S. W. Friedrich, B. A. Saville, and Y.-L. Cheng. Finite element modeling of drug distribution in the vitreous humor of the eye. *Invest. Ophthalmol. Vis. Sci* **37**:S582 (1996).
4. P. M. Pinksy, D. M. Maurice, and D. V. Datye. Finite element modeling of intravitreous drug kinetics. *Invest. Ophthalmol. Vis. Sci.* **37**:S700 (1996).
5. D. M. Maurice. Review: Practical issues in intravitreal drug delivery. *J. Ocular Pharm. Ther.* **17**:393–401 (2001).
6. J. C. Lang, R. E. Roehrs, D. P. Rodeheaver, P. J. Missel, R. Jani, and M. A. Chowhan. Design and evaluation of ophthalmic pharmaceutical products. In G. S. Banker (ed.), *Modern Pharmaceutics, 3rd ed., Revised and Expanded*, Marcel Dekker, New York, 2002, pp. 415–478.
7. The Anecortave Acetate Clinical Study Group. Anecortave Acetate as Monotherapy for the Treatment of Subfoveal Lesions in Patients with Exudative Age-Related Macular Degeneration (AMD): Interim (Month 6) Analysis of Clinical Safety and Efficacy. Retina (accepted).
8. P. J. Missel. Finite and infinitesimal representations of the vasculature: ocular drug clearance by vascular and hydraulic effects. *Ann. Biomed. Eng.* **30**: (2002).
9. P. J. Missel. Finite element modeling of diffusion and partitioning in biological systems: the infinite composite medium problem. *Ann. Biomed. Eng.* **28**:1307–1317 (2000).
10. T. E. Faber. *Fluid Dynamics for Physicists*, Cambridge University Press, Cambridge, 1995, p. 238.
11. D. J. Tritton. *Physical Fluid Dynamics*, Oxford University Press, Oxford, 1988, pp. 52–53.
12. B. Dhillon, A. Kamal, and C. Leen. Intravitreal sustained-release ganciclovir implantation to control cytomegalovirus retinitis in aids. *Int. J. STD & AIDS* **9**:227–230 (1998).
13. M. Araie and D. M. Maurice. The Loss of fluorescein, fluorescein glucoronide (FG) and fluorescein isothiocyanate dextran (FD) from the vitreous by the anterior and retinal pathways. *Exp. Eye Res.* **52**:27–39 (1991).
14. F. Johnson and D. Maurice. A simple method of measuring aqueous humor flow with intravitreal fluoresceinated dextrans. *Exp. Eye Res.* **39**:791–805 (1984).
15. M. R. Prausnitz and J. S. Noonan. Permeability of cornea, sclera, and conjunctiva: a literature analysis for drug delivery to the eye. *J. Pharm. Sci.* **87**:1479–1488 (1998).
16. T. W. Olsen, H. F. Edelhauser, J. I. Lim, and D. H. Geroski. Human scleral permeability: effects of age, cryotherapy, transscleral diode laser, and surgical thinning. *Invest. Ophthalmol. Vis. Sci.* **36**:1893–1903 (1995).
17. T. Krupin, L. F. Rosenberg, A. L. Sandridge, C. J. Bock, A. Berman, and J. M. Ruderman. Effects of topical k-strophanthin

on aqueous humor and corneal dynamics. *J. Glaucoma* **4**:327–333 (1995).
18. R. H. Funk, J. Gehr, and J. W. Rohen. Short-term hemodynamic changes in episcleral arteriovenous anastomoses correlate with venous pressure and IOP changes in the albino rabbit. *Curr. Eye Res.* **15**:87–93 (1996).
19. P. Blondeau, J. P. Tetrault, and C. Papamarkakis. Diurnal variation of episcleral venous pressure in healthy patients: a pilot study. *J. Glaucoma* **10**:18–24 (2001).
20. A. Bill. Uveoscleral drainage of aqueous humour in human eyes. *Exp. Eye Res.* **12**:275–281 (1971).
21. J. Cunha-Vaz and D. Maurice. Fluorescein dynamics in the eye. *Documenta Ophthalmol* **26**:61–72 (1969).
22. G. Backstrom. *Fluid Dynamics by Finite Element Analysis*, Studentlitteratur, Lund,1999; see for example Chapter 9, Viscous Flow in Channels.
23. M. Kaviany. *Principles of Heat Transfer in Porous Media,* Springer Verlag, New York, 1991, chapter 2.
24. D. M. Maurice. Flow of water between aqueous and vitreous compartments in the rabbit eye. *Am. J. Physiol.* **252**:F104–F108 (1987).
25. J. G. Cunha-Vaz and D. M. Maurice. The Active transport of fluorescein by the retinal vessels and the retina. *J. Physiol.* **191**: 467–486 (1967).
26. I. Fatt and B. Hedbys. Flow of water in the sclera. *Exp. Eye Res.* **10**:243–249 (1970).